Catalysis Communications 46 (2014) 17–21

Contents lists available at ScienceDirect

Catalysis Communications

journal homepage: www.elsevier.com/locate/catcom

Short Communication

Cu_2O/TiO_2 heterostructure nanotube arrays prepared by an electrodeposition method exhibiting enhanced photocatalytic activity for CO_2 reduction to methanol

Junyi Wang [a], Guangbin Ji [a,*], Yousong Liu [a], M.A. Gondal [b], Xiaofeng Chang [a]

[a] College of Material Science and Technology, Nanjing University of Aeronautics and Astronautics, Nanjing 211100, China
[b] Laser Research Group, Physics Department, Center of Excellence in Nanotechnology, King Fahd University of Petroleum and Minerals, Dhahran 31261, Saudi Arabia

ARTICLE INFO

Article history:
Received 13 June 2013
Received in revised form 21 September 2013
Accepted 12 November 2013
Available online 20 November 2013

Keywords:
Cu_2O/TiO_2 heterostructures
Electrodeposition
CO_2 photocatalytic reduction to methanol
Degradation of organic pollutants (dyes)

ABSTRACT

Cu_2O/TiO_2 composite nanotube arrays demonstrating enhanced photocatalytic performance were synthesized using an electrodeposition method to impregnate the p-type Cu_2O into the n-type titanium dioxide nanotube arrays (TNTs). The morphological results confirmed that the TNTs are wrapped by the Cu_2O nanoparticles and the UV–Vis absorption spectra showed that the Cu_2O/TNTs display a better ability for visible light absorption compared to the pure TNTs. CO_2 photocatalytic reduction experiments carried out by using Cu_2O/TNT nanocomposites proved that Cu_2O/TNTs exhibit high photocatalytic activity in conversion of CO_2 to methanol, while pure TNT arrays were almost inactive. Furthermore, Cu_2O/TNTs also exhibited augmented activity in degradation of target organic pollutant like acid orange (AO) under visible light irradiation. The ultra enhanced photocatalytic activity noticed by using Cu_2O/TNTs in CO_2 reduction and degradation of organic pollutant could be attributed to the formation of Cu_2O/TiO_2 heterostructures with higher charge separation efficiency.

1. Introduction

In recent years, a lot of research has been carried out to study the solar-driven photocatalytic conversion of CO_2 into hydrocarbon fuels to achieve the primary objective of the cyclic utilization of CO_2 due to global warming and climate change [1,2]. So far, semiconductor photocatalysts like TiO_2, ZnO [3], CdS [4], $ZnGa_2O_4$ [5], Zn_2GeO_4 [6,7], $InTaO_4$ [8], and WO_3 [9,10] have been widely investigated. Among them, TiO_2 has attracted considerable attention for its nontoxicity, low cost and stability in the field of photoelectric conversion and photocatalysis. Compared with the traditional TiO_2 particles, TiO_2 nanotube arrays have been widely applied for their large surface areas, excellent controllability, superior electron transport properties and excellent performance [11,12]. However, the wide band gap of TiO_2 (3.2 eV) inhibits its use for solar energy applications as TiO_2 only absorbs light having wavelength shorter than 387 nm in the ultraviolet region [13,14]. The construction of interface structure, such as heterojunction [15], is considered as an effective tool to improve the utilization of sun light and separation efficiency of the photo-generated electrons and holes. So far, the photocatalytic performance of the interface structures, such as CdS/TiO_2 [16], Fe_2O_3/TiO_2 [17], MoS_2 (WS_2)/TiO_2 [18], and CdS (Bi_2S_3)/TiO_2 [19], has been widely studied. Cu_2O exhibits great potential for applications in the field of the conversion of solar energy because of its advantages such as low price, visible light absorption and adjustable band-gap [20–24]. Coupled Cu_2O with TiO_2 to form Cu_2O/TiO_2 heterojunction may enhance the light absorption ability and photocatalytic activity in CO_2 reduction.

In this paper, we used TiO_2 nanotube arrays as the matrix to prepare Cu_2O/TNTs using electrodeposition method. The photoelectric properties and the photocatalytic activity of the composite photocatalyst in CO_2 reduction into hydrocarbon like methanol and photodegradation of organic pollutant (acid orange dye) were investigated.

2. Experimental section

2.1. Materials' preparation and characterization

Well-ordered TNTs were prepared by the anodization of Ti foil, as reported earlier [25]. The Cu_2O/TNT composites were prepared using a simple electrodeposition method (the preparation process in detail has been presented in the supplementary material). The morphology of the prepared samples was studied with scanning electronic microscopy (SEM, HITACHI-S4800). The crystal structure of the samples was examined by means of X-ray diffraction analysis (XRD, Bruker D8 ADVANCE with Cu-Kα radiation, $\lambda = 1.5418$ Å). UV–Vis absorption spectra of the Cu_2O/TNT composites were obtained using a UV–Vis spectrometer (Shimadzu UV-3600).

* Corresponding author. Tel.: +86 25 52112902; fax: +86 25 52112900.
E-mail address: gbji@nuaa.edu.cn (G. Ji).

1566-7367/$ – see front matter © 2013 Elsevier B.V. All rights reserved.
http://dx.doi.org/10.1016/j.catcom.2013.11.011

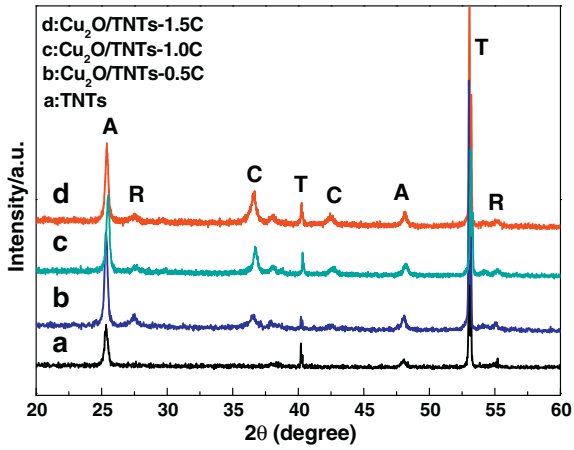

Fig. 1. XRD pattern of the prepared TNTs and Cu_2O/TNTs (A: Anatase, R: Rutile, C: Cu_2O, T: Ti substrate).

2.2. Photocatalytic reduction of CO_2

500 watt collimated xenon mercury (Xe Hg) broadband lamp (Oriel, USA) was used as the light source of excitation in this study. Catalyst was loaded in 100 mL distilled water in the reaction cell which could sustain 50 psi pressure without leaking. High purity CO_2 gas (99.99%) was introduced to the reactor and the reactor pressure was maintained at 50 psi. After a predetermined irradiation time, the liquid samples were withdrawn from the reactor by using syringe and were subjected to GC analysis. (The photocatalytic reduction process in detail has been presented in the supplementary material).

3. Results and discussion

3.1. Characterization

The phase structure of the Cu_2O/TNT samples was confirmed by the XRD results, as depicted in Fig. 1. The diffraction peaks of TNTs at

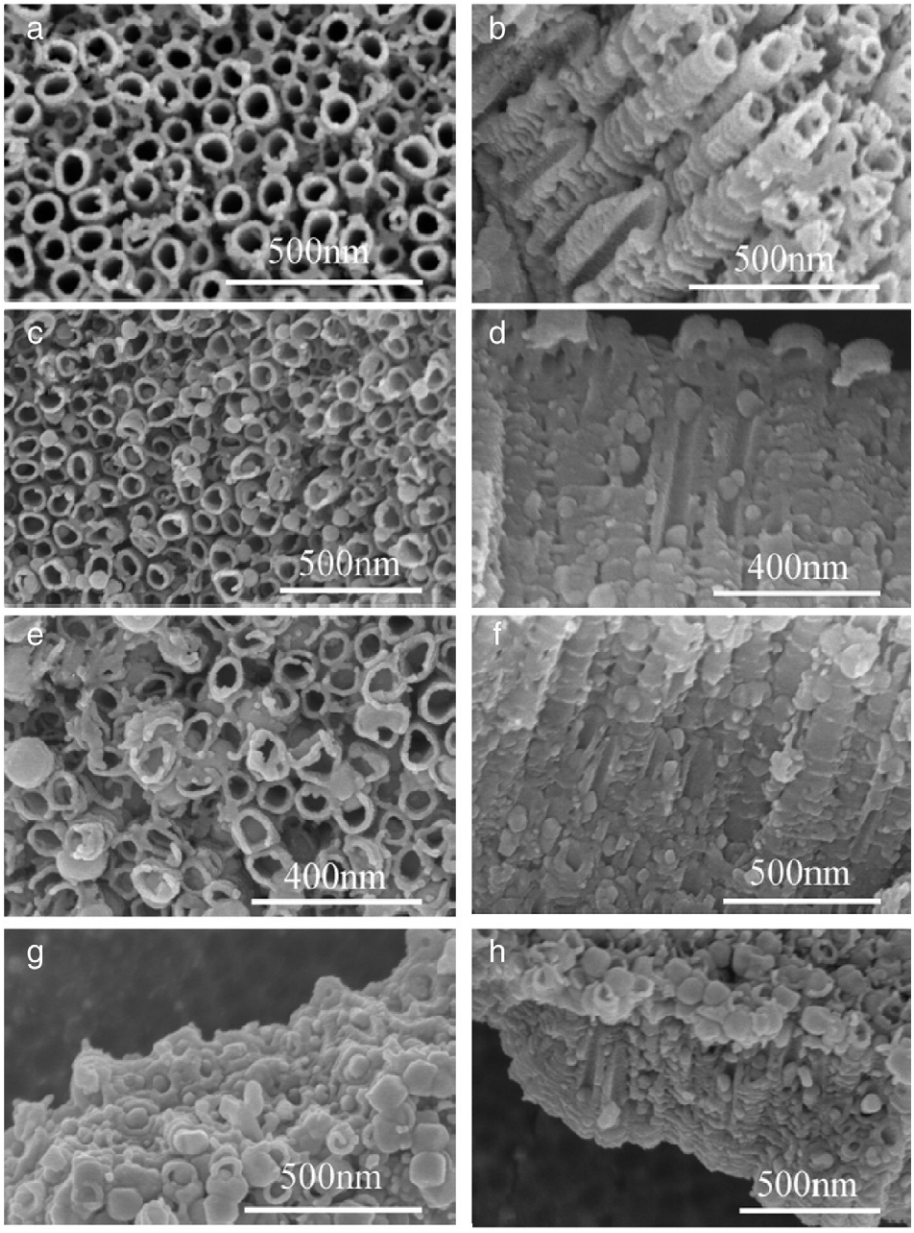

Fig. 2. SEM images of the TNTs and Cu_2O/TNTs with different electrodeposition charges: (a, b) TNTs, (c, d) 0.5 C, (e, f) 1.0 C and (g, h) 1.5 C.

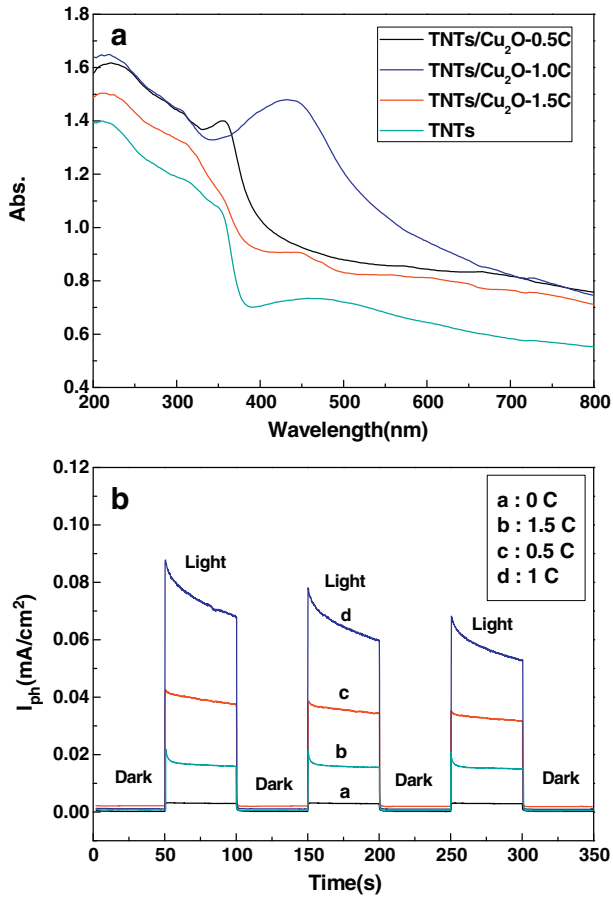

Fig. 3. UV–Vis DR spectra of the TNTs and Cu_2O/TNTs with different electrodeposition charges (a); Photocurrent density profiles of the TNTs and Cu_2O/TNTs at a bias potential of 0.0 V (vs. Ag/AgCl) under visible light (b).

25.3°and 48.0° can be assigned to (101) and (200) planes of TiO_2 having anatase phase (JCPDS Card No. 84-1286) and the diffraction peaks at 40.2° and 53.0° are indexed to the (101) and (102) planes of Ti substrate (JCPDS Card No. 44-1294), respectively. From the XRD curve of the Cu_2O/TNTs, it can be seen that the diffraction peaks at 27.4° could be assigned to (110) planes of TiO_2 of rutile phase (JCPDS Card No. 78-2485), suggesting that Cu_2O/TNT samples are consisted of anatase predominantly and a small amount of rutile. The diffraction peaks with 2θ values of 36.4 and 42.3 can be indexed to (111) and (200) planes of Cu_2O (JCPDS Card No.05-0667) respectively. With the deposition charge increases from 0.5 C to 1.5 C, the intensities of the Cu_2O characteristic peaks were also increased, which is resulted from the larger amount of the nanocrystalline Cu_2O deposited onto the nanotubes.

In Fig. 2a and b, SEM images illustrate that the TNTs are compact and the average inner diameter is approximately 80 nm having the length = 800 nm. From the top view (Fig 2c, e and g), the Cu_2O nanoparticles can be clearly noticed which are formed on the surface of the TNT arrays and the average side length of these Cu_2O nanoparticles with a polyhedral shape is about 80–100 nm. From the cross-sectional image view (Fig 2d, f and h), it is evident that the entire TNTs including the top, inner and outer walls of the TNTs are wrapped by the Cu_2O nanoparticles. By increasing the deposition charge from 0.5 to 1.0 C, the nanotube walls become rougher and rougher and the amount of the particles embedded into the structure seems also to be increasing. When the electrodeposition charges reach to 1.5 C, a large amount of Cu_2O nanoparticles arranges so compactly that they almost cover all the nanotube pores.

3.2. UV–Vis absorption spectra and photoelectrochemical results

From Fig. 3a it can be noticed that the adsorption intensity of the Cu_2O/TNT samples is clearly stronger than bare TNTs through the entire UV and visible light region, which demonstrate that the light absorption performance has been improved greatly due to the deposition of the Cu_2O nanoparticles. It also can be noticed that with the electrodeposition charge increasing, the adsorption intensity of the Cu_2O/TNT samples is increasing. However, the absorption intensity decreases when the electrodeposition charge reached 1.5 C, which could be attributed to the covered TiO_2 nanotubes with too much Cu_2O nanoparticles, which lead to the enhancement of the light reflection and the reduction of the light penetration into the TiO_2 nanotubes.

From the photoelectrochemical results (see Fig. 3b), one can see that there is no significant current in the dark, however, in the visible light illumination, the photocurrents of all the Cu_2O/TNT samples increase significantly while the bare TNTs showed negligible photoresponse. One can draw the conclusion that the photocurrent of Cu_2O/TNTs is greatly enhanced as compared with the TNTs, which may be ascribed to the photo-generated carrier separation efficiency of the Cu_2O/TNTs by taking the advantage of the formation of heterostructure. Therefore, it can be clearly inferred that the heterostructure construction is an effective way to improve the photoelectric performance.

3.3. Photocatalytic reduction of CO_2

In order to evaluate the photocatalytic activity of converting CO_2 into hydrocarbon fuels by TNTs and Cu_2O/TNTs, the conversion process was investigated by using high power pulsed laser as the light source. It is worth mentioning that laser excitation was a quite selective process for the end product like CH_3OH which is considered to be a future fuel in the CO_2 photocatalytic reduction. We selected the 1.0 C Cu_2O/TNTs, which exhibited the best photocatalytic activity in the CO_2 photocatalytic reduction process. Comparative tests demonstrated that very little product was found by using TNTs as photocatalysts, which is probably due to the low conductive band edge potential of TiO_2.

3.3.1. Analysis and quantification of methanol product

Gas chromatography (GC) peak positions using standard methanol and the calibration curve of methanol concentration vs GC peak area are depicted in Fig. S-1. As shown in Fig. 4a, after every 2 h irradiation for the Cu_2O/TNT sample, the GC peaks of methanol from CO_2 photoreduction are obtained. All the GC peaks appear at exactly 2.46 min retention time and no other GC peaks were detected, suggesting that the methanol is the only obtained product through the photocatalytic reduction of CO_2. Fig. 4a also depicts that as the irradiation time increase to 6 h, the GC methanol peak areas continuously grow to reach a maximum, which also indicates that the Cu_2O/TNT samples exhibit better photocatalytic activity than that of the TNTs. Fig. 4b depicts the concentration and conversion efficiency trend of CO_2 photoreduction into methanol as a function of irradiation time. It demonstrates that the concentration of methanol increases with the irradiation time and reaches to its maximum (55.15 μM/100 mL) at 6 h.

3.3.2. Conversion and photonic efficiency of CO_2

The efficiency for CO_2 conversion into methanol using Cu_2O/TNTs was also calculated. In a typical experiment, an amount of CO_2 dissolved in 1 L distilled water at atmospheric pressure is 34 mmol, as calculated by Henry's law. The CO_2 pressure in our experiments was 50 psi (3.4 atm), so the amount of CO_2 dissolved in 100 mL water would be 11.56 mmol. The CO_2 conversion efficiency can be estimated by the ratio of the methanol concentration to CO_2 concentration. As depicted in Fig. 4b, the maximum concentration of methanol is 55.15 uM/100 mL and the maximum CO_2 conversion efficiency is about 0.48% after 6 h irradiation.

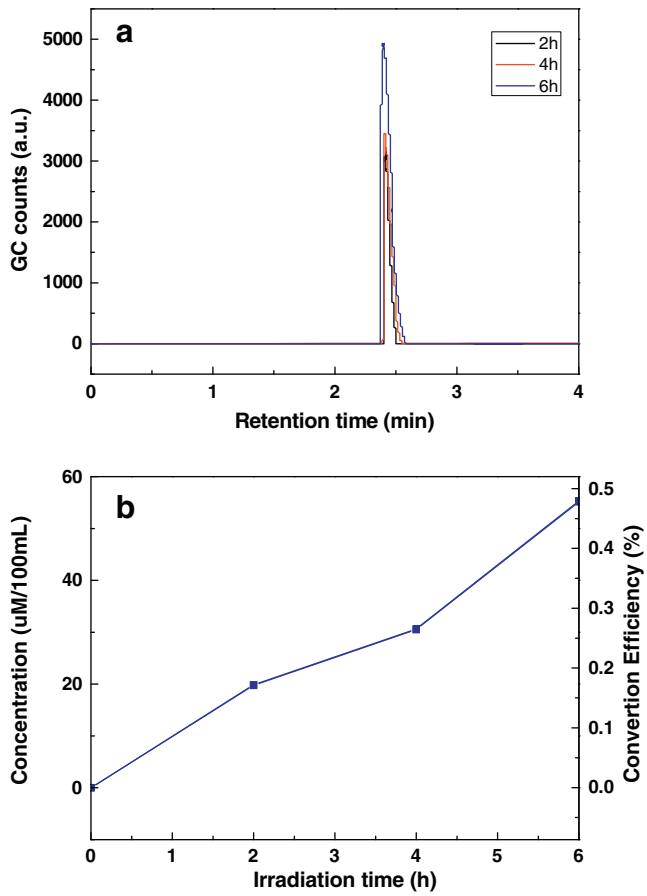

Fig. 4. GC peaks of methanol taken after every 2 h interval irradiation with a laser pulse energy of 40 mJ/pulse at 355 nm radiation and catalyst in 100 mL distilled water, with 50 psi CO_2 pressure (a); Concentration and conversion efficiency of produced CH_3OH (b).

Moreover, the photonic efficiency of CO_2 conversion into methanol using Cu_2O/TNTs was also investigated. The number of methanol molecules can be calculated from the product molar concentration and Avogadro number. The photon number can be calculated to be 4.286×10^{19} photons/min. The maximum rate of methanol production is 1.2366×10^{17} molecules/min at the irradiation time interval from 4 to 6 h. As a single methanol molecule needs 6 photogenerated electrons, the maximum photonic efficiency of CO_2 photoreduction can be computed $6 \times 1.2366 \times 10^{17} / 4.286 \times 10^{19}$ to be about 1.731%. To the best of our knowledge, the high photonic efficiency of Cu_2O/TNTs may be due to the construction of Cu_2O/TNT heterojunction.

3.4. Photocatalytic activity for the degradation of AO

In order to further prove the construction of Cu_2O/TiO_2 heterojunction, the photocatalytic activity of the samples was evaluated by the degradation of AO. The Cu_2O/TNT samples exhibit enhanced catalytic activity that 90% of the AO was photocatalytically degraded using the 1.0 C Cu_2O/TNTs and only 20% of the AO was decolorized by the bare TNTs after 2 h of visible light irradiation. The photocatalytic results of using Cu_2O/TNT samples with different electrodeposition charges and the repeated photocatalytic degradation with 1.0 C Cu_2O/TNTs are depicted in Fig. S-2 to S-6.

3.5. Possible mechanism for the improved photocatalytic property of Cu_2O/TNTs

For the Cu_2O/TiO_2 composite system under visible light irradiation, only the electrons in Cu_2O are excited to the conduction band. In the excitation process, as the Cu_2O potentials of both conduction band and valence band are more negative than that of TiO_2, the photo-generated electrons in the conduction band of Cu_2O particles transfer to the TiO_2, leading to the spatial separation of the photo-generated holes and electrons. Under the irradiation of ultraviolet–visible light, the electrons both in Cu_2O and TiO_2 are excited to the conduction band. Photo-generated electrons in conduction band of Cu_2O particles quickly transfer to TiO_2 particles, whereas photo-generated holes in valence band of TiO_2 particles migrate to the surface of Cu_2O particles. The separation of electrons and holes reduces the charge recombination rate and thus promotes eventually the photocatalytic activity. The schematic charge separation in the Cu_2O/TiO_2 heterojunction structure is depicted in Fig. 5.

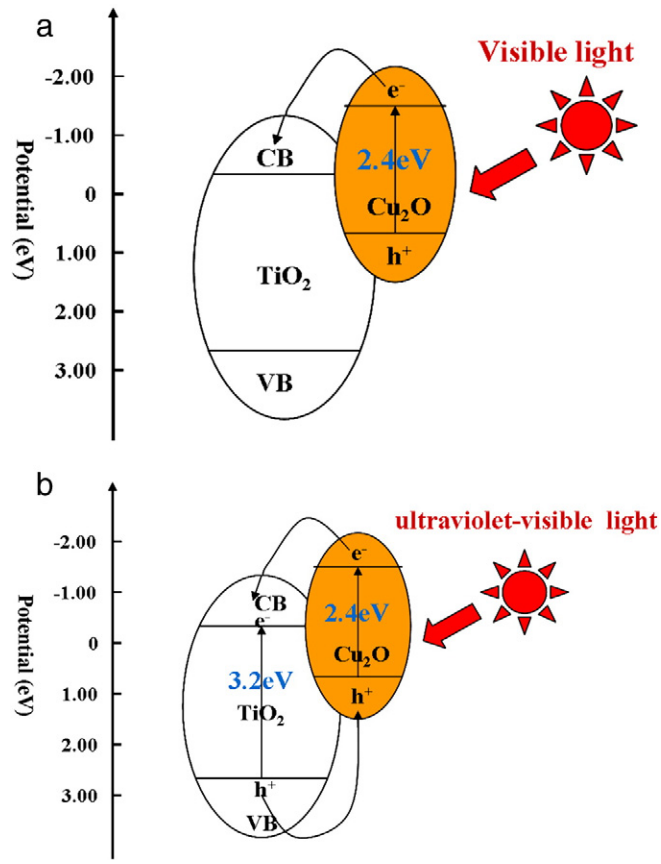

Fig. 5. A schematic of the charge separation in Cu_2O/TiO_2 heterojunction structure catalysts under visible light irradiation (a); ultraviolet–visible light irradiation (b).

4. Conclusion

In summary, Cu_2O/TNTs have been prepared successfully through the electrodeposition method. The Cu_2O/TNT composites exhibit much higher photocatalytic activity than bare TNTs for the CO_2 conversion into methanol and degradation of AO under light irradiation, which may be due to the formation of Cu_2O/TiO_2 heterostructure and higher charge separation efficiency. Furthermore, such nanocomposite material may bring a new insight into the design and applications of highly efficient photocatalysts.

Acknowledgments

The work is financially supported by the National Natural Science Foundation of China (No. 51172109) and Jiangsu province Natural Science Foundation (No. BK2010497). Prof. Gondal is thankful to KFUPM for supporting this work under project #RG1011-1/2.

Appendix A. Supplementary data

Supplementary data to this article can be found online at http://dx.doi.org/10.1016/j.catcom.2013.11.011.

References

[1] G.S. Shao, F.Y. Wang, T.Z. Ren, Y.P. Liu, Z.Y. Yuan, Appl. Catal. B 92 (2009) 61–67.
[2] G.S. Shao, L. Liu, T.Y. Ma, F.Y. Wang, T.Z. Ren, Z.Y. Yuan, Chem. Eng. J. 160 (2010) 370–377.
[3] F.C. Meunier, Angew. Chem. Int. Ed. 50 (2011) 4053–4054.
[4] Y.S. Chaudhary, T.W. Woolerton, C.S. Allen, J.H. Warner, E. Pierce, S.W. Ragsdale, F.A. Armstrong, Chem. Commun. 48 (2012) 58–60.
[5] S.C. Yan, S.X. Ouyang, J. Gao, M. Yang, J.Y. Feng, X.X. Fan, L.J. Wan, Z.S. Li, J.H. Ye, Y. Zhou, Angew. Chem. Int. Ed. 49 (2010) 6400–6404.
[6] Q. Liu, Y. Zhou, J.H. Kou, X.Y. Chen, Z.P. Tian, J. Gao, S.C. Yan, J. Am. Chem. Soc. 132 (2010) 14385–14387.
[7] N. Zhang, S.X. Ouyang, T. Kako, J.H. Ye, Chem. Commun. 48 (2012) 1269–1271.
[8] H.C. Chen, H.C. Chou, J.C.S. Wu, H.Y. Lin, J. Mater. Res. 23 (2008) 1364–1370.
[9] P. Maruthamuthu, M. Ashokkomar, K. Gurunathan, E. Subramanian, M.V.C. Shastri, Int. J. Hydrogen Energy 14 (1989) 525–528.
[10] P. Maruthamuthu, M. Ashokkomar, Int. J. Hydrogen Energy 14 (1989) 275–277.
[11] I. Paramasivalm, J.M. Macak, P. Schmuki, Electrochem. Commun. 10 (2008) 71–75.
[12] J.M. Macak, M. Zlamal, J. Krysa, P. Schmuki, Small 3 (2007) 300–304.
[13] K.H. Yoo, K.S. Kang, Y. Chen, K.J. Han, J. Kim, Nanotechnology 19 (2008) 505202.
[14] H.J. Zhang, G.H. Chen, D.W. Bahneman, J. Mater. Chem. 19 (2009) 5089–5121.
[15] Z.Y. Zhang, C.L. Shao, X.H. Li, C.H. Wang, M.Y. Zhang, M.Y. Zhang, Y.C. Liu, ACS Appl. Mater. Interfaces 2 (2010) 2915–2923.
[16] S. Banerjee, S.K. Mohapatra, P.P. Da, M. Misra, Chem. Mater. 20 (2008) 6784–6791.
[17] A.I. Kontos, V. Likodimos, T. Stergiopoulos, D.S. Tsoukleris, P. Falaras, Chem. Mater. 21 (2009) 662–672.
[18] W. Ho, J.C. Yu, J. Lin, J. Yu, P. Li, Langmuir 20 (2004) 5865–5869.
[19] X. Li, H. Liu, D. Luo, J. Li, Y. Huang, H. Li, Y. Fang, Y. Xu, L. Zhu, Chem. Eng. J. 180 (2012) 151–158.
[20] C.H. Lu, L.M. Qi, J.H. Yang, Adv. Mater. 17 (2005) 2562–2567.
[21] W. Siripala, A. Ivanovskaya, T.F. Jaramillo, Sol. Energy Mater. Sol. Cells 77 (2003) 229–237.
[22] H.M. Yang, J. Ouyang, A.D. Tang, Mater. Res. Bull. 41 (2006) 1310–1318.
[23] J.L. Li, L. Liu, Y. Yu, Electrochem. Commun. 6 (2004) 940–943.
[24] H.L. Li, Y.G. Lei, Y. Huang, Y.P. Fang, Y.H. Xu, L. Zhu, X. Li, J. Nat. Gas Chem. 20 (2011) 145–150.
[25] J.H. Yun, Y.H. Ng, C. Ye, A.J. Mozer, G.G. Wallace, ACS Appl. Mater. Interfaces 3 (2011) 1585–1593.